Fully Automated Reduction of Ocular Artifacts in High-Dimensional Neural Data

John W. Kelly*, *Student Member, IEEE*, Daniel P. Siewiorek, *Fellow, IEEE*, Asim Smailagic, *Fellow, IEEE*, Jennifer L. Collinger, Douglas J. Weber, *Member, IEEE*, and Wei Wang

***Abstract*—The reduction of artifacts in neural data is a key element in improving analysis of brain recordings and the development of effective brain–computer interfaces. This complex problem becomes even more difficult as the number of channels in the neural recording is increased. Here, new techniques based on wavelet thresholding and independent component analysis (ICA) are developed for use in high-dimensional neural data. The wavelet technique uses a discrete wavelet transform with a Haar basis function to localize artifacts in both time and frequency before removing them with thresholding. Wavelet decomposition level is automatically selected based on the smoothness of artifactual wavelet approximation coefficients. The ICA method separates the signal into independent components, detects artifactual components by measuring the offset between the mean and median of each component, and then removing the correct number of components based on the aforementioned offset and the power of the reconstructed signal. A quantitative method for evaluating these techniques is also presented. Through this evaluation, the novel adaptation of wavelet thresholding is shown to produce superior reduction of ocular artifacts when compared to regression, principal component analysis, and ICA.**

***Index Terms*—Artifact removal, electrooculographic (EOG), independent component analysis (ICA), magnetoencephalography (MEG), neural data, wavelet thresholding.**

I. Introduction

THE STUDY of human brain function can benefit both engineering and medicine. Clinical neural monitoring is critical in diagnosing and treating many neurological disorders such as epilepsy. Brain–computer interfaces (BCIs) present the possibility of creating a direct link between humans and their environment, allowing the use of brain-controlled devices to assist people with disabilities.

One problem in neural signal processing is the presence of noise and artifacts in neural recordings. Major artifacts can come from a variety of sources, including eye movement, muscle movement, cardiac rhythm, outside sources, and even neural processes other than the one of interest [1]. Artifacts produced by eye movement and blinks, which are commonly referred to as ocular artifacts (OA) or electrooculographic (EOG) artifacts, are typically dominant over other electrophysiological artifacts.

Many methods have been attempted for artifact removal [2]. A common practice has always been to simply reject data contaminated with artifacts. For many forms of clinical monitoring, this is acceptable because there is an abundance of data, but in BCI research and in many other neural studies, a scarcity of data or a high percentage of contamination makes this method unusable. Another classic solution for dealing with EOG artifacts is to instruct the person to avoid eye movement and blinking. For some situations this may not be possible, and it has also been shown that avoiding blinks introduces a cognitive process in the brain [3], [4]. This method then removes EOG artifacts while creating neural artifacts.

The only consistently viable solutions for dealing with artifacts are to either remove them or, in the case of BCIs, to develop decoding algorithms that are invariant to them. The latter method is not always possible, though. Also, it is difficult to prove invariance without an artifact-free signal for comparison. Thus, artifact removal is highly beneficial to both BCI and general neuroscience research [2], [5].

In part due to advances in neural recording techniques and computing power, the dimensionality available in neural data has steadily increased. High-dimensional data are useful for clinical studies as well as for BCI and neuroscience research, but they can make artifact removal more difficult. In this paper, artifact removal methods are evaluated on high-dimensional magnetoencephalography (MEG) data. The data not only demonstrate

Manuscript received May 28, 2010; revised September 18, 2010; accepted October 22, 2010. Date of publication November 22, 2010; date of current version February 18, 2011. The work of J. W. Kelly was supported by a National Defense Science and Engineering Graduate Fellowship, sponsored by the Air Force Office of Scientific Research, an NSF Graduate Research Fellowship, and the Quality of Life Technology Center under NSF Grant EEEC-0540865. This work was supported in part by the NSF under Cooperative Agreement EEC-0540865, in part by the Telemedicine and Advanced Technology Research Center (TATRC) of the U.S. Army Medical Research and Materiel Command Agreement W81XWH-07-1-0716, in part by the National Center for Research Resources (NCRR) under Grant 5UL1RR024153, in part by the Office of Research and Development, Rehabilitation Research and Development Service, VA Center of Excellence in Wheelchairs and Associated Rehab Engineering under Grants B3142C and B6789C, in part by a special grant from the Office of the Senior Vice Chancellor for the Health Sciences at the University of Pittsburgh, and in part by the NIH grants from the NIBIB (1R01EB007749) and NINDS (1R21NS056136). *Asterisk indicates corresponding author.*

*J. W. Kelly is with the Department of Electrical and Computer Engineering, Carnegie Mellon University, Pittsburgh, PA 15213 USA (e-mail: jwkelly@cmu.edu).

D. P. Siewiorek and A. Smailagic are with the Department of Electrical and Computer Engineering, Carnegie Mellon University, Pittsburgh, PA 15213 USA (e-mail: dps@cs.cmu.edu; asim@cs.cmu.edu).

J. L. Collinger is with the Department of Physical Medicine and Rehabilitation, University of Pittsburgh, Pittsburgh, PA 15213 USA, and also with the Human Engineering Research Laboratories, Department of Veterans Affairs, Pittsburgh, PA 15213 USA (e-mail: collingr@pitt.edu).

D. J. Weber and W. Wang are with the Department of Physical Medicine and Rehabilitation, University of Pittsburgh, Pittsburgh, PA 15213 USA (e-mail: djw50@pitt.edu; wangwei3@pitt.edu).

Digital Object Identifier 10.1109/TBME.2010.2093932

0018-9294/$26.00 © 2011 IEEE

the feasibility of the techniques on high-dimensional data, but also ensure that removal methods are evaluated across nearly the entire surface of the brain. The goal of this paper is to demonstrate novel EOG removal techniques on these data and establish their effectiveness through a quantitative comparison to traditional removal methods.

The first novel technique uses a discrete wavelet transform with a Haar basis function to localize artifacts in both time and frequency before removing them with thresholding. A multilevel wavelet method was developed in order to automatically select the level of decomposition for optimal time–frequency isolation of artifacts. This method is based on the smoothness of the artifactual approximation coefficients.

The second novel method separates the signal into independent components and labels some as artifactual by a method termed distribution offset, which measures the difference between the mean and the median of each component. The correct number of components is removed based on distribution offset and the power of the reconstructed signal.

A major challenge with artifact reduction in neural data is evaluating the results [6]. Since the true, artifact-free neural signal is not known, it is difficult to quantitatively assess the performance of artifact removal techniques. In simulated data this truth is known, but simulations do not fully capture the nature of neural recordings. An automated quantitative method for determining the success of artifact reduction in real data is needed. Such a method was developed here based on correlation, Euclidean distance, and the difference in power between the signal before and after EOG removal, as well as the number of detected artifacts before and after removal. These metrics attempt to measure the effectiveness of the techniques in removing artifacts while preserving neural data.

For comparison to the novel EOG removal techniques, a few traditional methods based on regression, principal component analysis (PCA), and independent component analysis (ICA) were also analyzed. The background for methods used in this paper is presented in Section II and the implementation of these methods is given in Section III. The results and discussion are in Section IV and the conclusion is in Section V.

II. Background

A. EOG Artifact Removal Techniques

Neural recordings can be modeled as follows:

$$\boldsymbol{X} = \boldsymbol{S} + \boldsymbol{A} * \boldsymbol{N} \tag{1}$$

where the matrix $\boldsymbol{X}$ (m by k) is the neural recording, $\boldsymbol{S}$ (m by k) contains the actual neural activity at the sites of the recording, $\boldsymbol{N}$ (p by k) is the noise, and $\boldsymbol{A}$ (m by p) determines the contribution of each noise source to each channel of recorded data. m is the number of neural recording channels, k is the number of samples, and p is the number of noise sources. Here, it will be assumed that the source of noise is eye movement so $\boldsymbol{A}$ will be null for the columns of all other noise sources. Three types of EOG artifacts must be accounted for the following: 1) saccadic artifacts produce a near box-shaped waveform; 2) blink artifacts produce a sharp spike; and 3) normal eye movement resembles a low frequency drift. EOG artifacts occupy a fairly wide frequency band, but are generally strongest under 4 Hz [7].

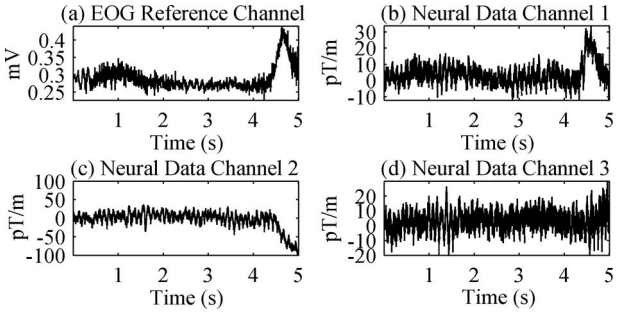

Fig. 1. Effect of EOG artifact on (a) EOG reference channel and (b)–(d) three neural recording channels. (b) Eye blink artifact is nearly duplicated, (c) artifact's effect has opposite polarity and appears slightly delayed, and (d) no obvious effect is visible. Note that the neural channel numbers in this figure have no spatial relevance.

It is often possible to obtain a model for an ocular artifact through EOG reference channels. EOG artifacts occur because the cornea and retina are oppositely charged, causing the eye to be a dipole. Movement of this dipole creates a large change in potential that propagates across the scalp, contaminating neural recordings. EOG reference channels attempt to measure this contamination at the source with electrodes placed above and below and to either side of the eye (to account for both horizontal and vertical eye movements). Sometimes electrodes are also used to measure radial eye movement.

Since it is possible to obtain a model for the noise through EOG recordings, (1) leads naturally to the use of regression to remove the artifact from the recorded signal. $\boldsymbol{N}$ is approximated by the EOG channels, and then it is only necessary to calculate $\boldsymbol{A}$ to solve for $\boldsymbol{S}$ in (1). The problem with the regression method is that it assumes that the EOG recordings are clean models. In reality, the contamination is bidirectional and a small amount of neural data propagates to the sites of the EOG recordings. In subtracting out the EOG signals, some neural information is then lost. Also, neural data that propagate to reference channels are introduced into other recording sites [8].

With correlation between the clean neural signal and the EOG recording, it is actually impossible to solve for an exact value of $\boldsymbol{A}$ in the regression model. Even methods that utilize a topographic map of electrical propagation from the eyes across the scalp fail due to the inherent variance in such a map caused by skin and environmental conditions. An EOG artifact can also affect neural channels in different ways, as shown in Fig. 1.

Another approach for EOG artifact reduction is component-based methods such as PCA and ICA. The goal in these methods is to: 1) transform the original signal into a component space; 2) identify components that correspond to artifacts; and then 3) transform back to the original data space using only nonartifactual components. This process is shown in Fig. 2.

PCA transforms a dataset into uncorrelated components and sorts them in order of the amount of variance each component contributes to the dataset. In the context of noise removal, PCA can be useful in multichannel datasets in which the same source

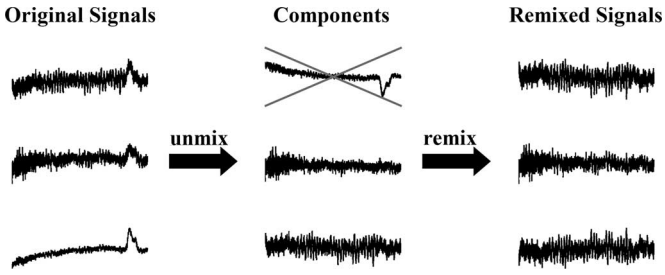

Fig. 2. Illustration of component-based artifact removal process. Here, the eye blink artifact seen near the end of the signals is isolated to the top component when the signals are transformed to the component space. The columns are nulled that correspond to this component in the matrix used for transforming the components back to the signal space, so this component is removed from the original signal.

of noise is contaminating all channels, especially if the noise has a higher amplitude than the signal. This has been shown to be effective in EOG removal [9]. For this process, the somewhat arbitrary assumption must be made that the signal sources are spatially orthogonal. Also, while PCA does decorrelate the signals, it does not guarantee independence.

ICA is able to achieve independence between components. It is also one of the most highly studied and successful techniques for artifact removal in neural signals [15], [17]–[19]. Neural recordings (other than single-neuron recordings) consist of a mixture of signal sources at each recording site, so the problem of removing EOG artifacts can be modeled as a blind source separation problem. ICA separates the sources by maximizing independence based on one of a number of possible metrics. A few assumptions are made when using standard ICA, the most important here being that at most one of the sources is Gaussian and that there is negligible signal propagation delay. ICA is also unable to determine the correct order, scale, or polarity of the sources, making artifact identification difficult.

The final method examined in this paper uses wavelet decomposition for EOG removal. This technique has received much less attention in the research community, but some work has been done [10], [11] and wavelets have been applied in other areas of neural signal processing [12], [13].

Wavelet decomposition involves recursively passing the signal through a pair of quadrature mirror filters and downsampling, resulting in the coefficients at each level of decomposition having higher frequency resolution and lower temporal resolution than the previous level. The goal in removing artifacts with wavelet decomposition is normally to isolate the artifact so that it can be removed with a thresholding function. This can be done by attempting to match the shape of the wavelet to the transient of interest, which is an EOG artifact in this case, or by trying to isolate an artifact based on its time–frequency localization. In either case, the isolated artifact can then be removed with thresholding before reconstructing the signal. Typically, this technique does not need a template for the noise channel and it is also fairly easy to automate, but its performance depends largely on the choice of threshold, basis function, and decomposition level.

B. Evaluation of Artifact Reduction

Providing a quantitative evaluation for artifact removal is a difficult problem in itself. With recorded neural data, it is difficult to even estimate the artifact-free signal since neural signals are nonstationary. This means that there is no ground truth to use for comparison with the processed signal.

If the ground truth is known, such as in simulated data, there are methods to evaluate the results of EOG removal. Some of these measures are the correlation coefficient, the ratio of the standard deviation (STD), and the Euclidean distance between the processed signal and the true, artifact-free signal [14]. The correlation coefficient determines how well the shape of the true signal is retained, the STD ratio determines how much the power is affected, and the Euclidean distance helps measure both shape and amplitude. The closer the correlation coefficient and STD ratio are to 1 and the closer the Euclidean distance is to 0, the better the results of the EOG removal. These methods must be adapted for use on real data, though.

Another common evaluation criterion is to look at frequency correlation (2) [10]. In (2), $\tilde{x}$ and $\tilde{y}$ are the Fourier coefficients of the two signals, and w_1 and w_2 are bounds of the frequency window. This measure is just a windowed version of coherence. The goal is to show that the processed signal is nearly perfectly correlated with the original signal at all frequencies except the band containing the artifact.

$$c_{x,y} = \frac{0.5 \cdot \sum_{w1}^{w2} \tilde{x}^* \tilde{y} + \tilde{x} \tilde{y}^*}{\sqrt{\sum_{w1}^{w2} \tilde{x}\tilde{x}^* \cdot \sum_{w1}^{w2} \tilde{y}\tilde{y}^*}}. \tag{2}$$

III. Methods

As stated earlier, high-dimensional neural data can be extremely useful in clinical studies and in both BCI and neuroscience research. The methods presented here overcome the unique problems encountered in removing EOG artifacts from high-dimensional data. Both novel and traditional EOG removal methods based on regression, component analysis, and wavelets were implemented. The performance of these methods was analyzed using automated, quantitative metrics that are also presented here. All methods were fully automated and computation time was measured, as speed and automation are important in high-dimensional data.

A. Regression-Based Removal

The first removal method examined was regression. As stated in Section II, regression attempts to calculate $\boldsymbol{A}$ in (1) in order to solve for $\boldsymbol{S}$. Many algorithms have been used in solving for $\boldsymbol{A}$, and the one used here is given by (3). This equation can be proven under the false, but necessary assumption that the correlation between the EOG reference channel $\boldsymbol{N}$ and the clean neural signal $\boldsymbol{S}$ is zero [14]. Note that in (3), X_m and N_p are zero mean and the ratio is the estimations at zero lag of the cross covariance between X_m and N_p and the autocovariance

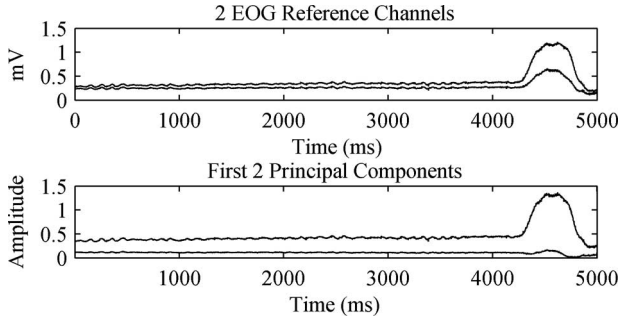

Fig. 3. EOG reference channels and corresponding principal components. PCA was run on the full data matrix of EOG reference channels and neural data channels. Most of this saccadic movement artifact is accounted for by the first principal component since the EOG channels are highly correlated.

of N_p.

$$A_{m,\,p} = \frac{X_m \cdot N_p^T}{N_p \cdot N_p^T}. \tag{3}$$

Here, it was assumed that $\boldsymbol{A}$ was the same for multiple EOG channels (i.e., $A_{m,i} = A_{m,j}$ for all i, j), so in (3) p was set to 1 and N_1 equaled the sum of the EOG channels. This was a reasonable assumption for the purposes of this study since the source, and thus the propagation path, of the EOG channels was the same. Since $\boldsymbol{A}$ was calculated algorithmically, this removal method was fully automated.

B. Component-Based Removal

With high-dimensional data, PCA and ICA became difficult since they perform computations on all channels at once. With PCA the computations were still possible, but it was at times difficult to load the necessary data into memory at once.

Like regression, PCA was simple to automate. This was mostly due to the high amplitude of EOG artifacts relative to neural signals. Since the artifact was distributed throughout the neural data at various scales, the high amplitude caused the artifact to contribute a large amount of variance to the data. In the absence of other high-amplitude artifacts such as interictal spikes in subjects with epilepsy, it was fairly safe to assume then that any artifactual components would contribute the highest amount of variance to the data. Since PCA orders components by variance, the first p principal components should then contain the artifacts, where p is the number of EOG channels (Fig. 3). In transforming the components back to the original signal space, the first p columns of the transformation matrix were nulled.

ICA faced the most difficulties with high-dimensional data. In order for ICA to converge, the number of time points usually needs to be at least several times the square of the number of data channels [15]. For high-dimensional data, the number of time points needed often exceeds trial length.

Two solutions were considered for allowing ICA to converge. First, multiple trials could be concatenated to achieve enough time points. This method assumes that the neural sources and the linear mixture model are stationary across trials. Second, a separate epoch of ICA could be run for each neural data channel paired with the EOG reference channels, as opposed to doing one epoch of ICA containing all the data channels. This is a very time-consuming process, but it also has a few beneficial side effects such as less of a need to worry about the mixtures of distinct neural processes at each electrode, i.e., spatial stationarity of the underlying neural sources, linearity of the mixtures, and the number of sources. Here, the latter of the two methods was used. This is because different trials in the data could contain different stimuli, and thus, it would be unknown if the neural sources would remain stationary across trials. To somewhat alleviate the problem of computation time, the fast ICA algorithm was used [16].

A further difficulty in using ICA on high-dimensional data was automating the process of identifying artifactual components. Many studies using ICA manually identify artifacts through visual inspection [17], but for a large dataset that would be impractical. Multiple methods for automation have been examined, such as the Hurst exponent [18], kurtosis, Shannon's entropy, and Renyi's entropy [19]. Unfortunately, Renyi's entropy proved too computationally costly for high-dimensional data due to the kernel density estimation necessary for each component. The Hurst exponent was used, and the results were compared to a novel method for identifying artifactual components. For the Hurst exponent method, removing components with Hurst values in the eye blink range of 0.58–0.64 removed very few artifacts, so only components with values of 0.70–0.76 that correspond to data from actual neural processes were kept while all others were marked as artifacts. These values are described further in [18].

The novel artifactual component identification method, which will be referred to as the distribution offset, ranks each component by its chances of being an artifactual component. The high amplitude of an artifact causes the mean of the component's distribution to be offset from its median. The mean of a clean neural signal, even one in the presence of a strong event-related potential, will not be offset nearly as much. To calculate the distribution offset, the component was centered, and then the difference between the number of samples on the same side of zero and half the number of time points was calculated. This is shown in (4), where k is the number of samples and C is the independent component. This measure is similar to skewness, but skewness also factors in the distances of points from the mean.

$$\left| \frac{k}{2} - \sum_{i=1}^{k} y_i \right|, \qquad y_i = \begin{cases} 1, & C_i - E[C] > 0 \\ 0, & \text{otherwise} \end{cases}. \tag{4}$$

The distribution offset was used to initially mark artifactual components as those where the value in (4) was more than 3% of the number of samples. The columns in the mixing matrix were nulled that corresponded to these components. As is the case in Fig. 4, the distribution offset normally made a good distinction between artifactual component and neural component, but an additional step was taken since a small number of components leave little room for error in the number of components removed.

After remixing, if the signal's power was far above the power of a normal neural signal, then the component with the next highest distribution offset was removed. Likewise, if the resulting

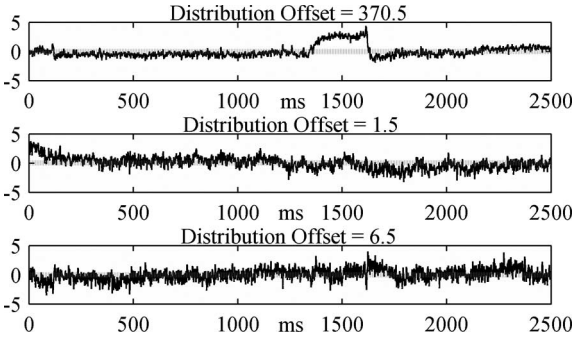

Fig. 4. Distribution offset values for components of one epoch of ICA. The top component is artifactual, as is detected by the distribution offset. The gray dotted line represents the signal mean.

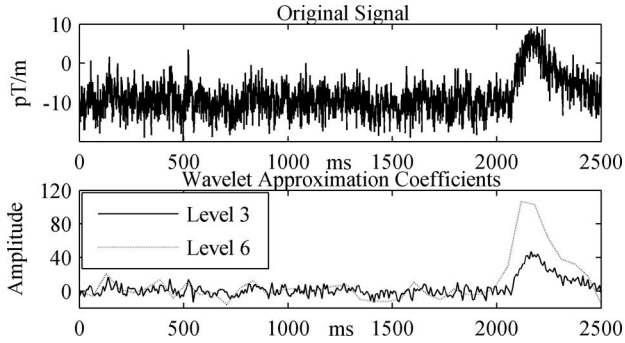

Fig. 5. Wavelet approximation coefficients at two decomposition levels. Level 3 and level 6 were used to accentuate the differences between levels of decomposition. Here, the level 3 decomposition still contains neural data, and the level 6 decomposition has stretched the artifact's temporal bounds.

signal power was far below the power of a normal neural signal, the removed component with the lowest distribution offset was added back to create the final signal. Acceptable power levels corresponded to a STD between 1e−15 and 1e−11, although these thresholds could vary with neural recording method. This procedure was also used with the Hurst exponent method, with the distance of the exponent from 0.73 as the ranking criteria.

C. Wavelet-Based Removal

The wavelet approach used here was a novel method that took advantage of the fact that EOG artifacts are well localized in time and frequency. The traditional discrete wavelet transform was used with the goal of isolating the artifact in both time and frequency in order to minimize the impact of the artifact removal process on the rest of the neural signal. As in other wavelet techniques, the wavelet coefficients were thresholded to remove the artifact before reconstructing the signal from the thresholded coefficients.

For the wavelet basis function, the Haar wavelet was chosen as it is the simplest wavelet and computation time is important on high-dimensional data. The Haar wavelet provides accurate decomposition and reconstruction with minimum distortions and data redundance [20]. Also, many of its limitations, such as nondifferentiability and a chance for detail coefficients to miss sudden changes, were not a concern here as we were examining approximation coefficients and then simply thresholding and reconstructing the data. The strategy of selecting a wavelet that matches the shape of the transient of interest was not used since the three types of EOG artifacts have markedly different shapes.

To localize the artifact, it is important to zoom in just the right amount in time and frequency. This was done by selecting the proper level of wavelet decomposition. Each level of decomposition increases frequency resolution and decreases temporal resolution. Decompose too far and the artifact will be diluted across frequency bands making it difficult to remove with thresholding and difficult to isolate in time. Decompose too little and the artifact will not be isolated in frequency, causing neural data to be unnecessarily lost in the thresholding process. This is shown in Fig. 5, where the level 3 decomposition failed to isolate the artifact in frequency and the level 6 decomposition began to stretch the temporal bounds of the artifact. The proper level of decomposition depends in large part on whether the artifact is the result of a blink, or of saccadic or regular eye movement, and also on the sampling frequency of the data.

To choose the proper decomposition level for each artifact, a strategy of multilevel wavelet decomposition was used. If an artifact has been fully isolated, its wavelet coefficients should be smooth, but cross contamination with neural signals can make it appear to have higher frequency components (Fig. 5). The multilevel process attempts to continue the wavelet decomposition to a depth that is sufficient to remove these higher frequency components.

In this process, the signal first underwent a minimum level wavelet decomposition, which was set at level 3. The bounds of any EOG artifacts were then marked by locating threshold crossings and finding the first local extrema on the outside of those crossings. The threshold was $\pm$ (5e−11 + |median(A)|), where A is the vector of wavelet coefficients, although the optimal value of this threshold could again vary with recording method. To determine smoothness, it was checked if the derivative of the artifactual coefficients ever changed sign on either side of the peak. If it did, neural data were assumed to still be present and the wavelet decomposition went a level deeper. The artifactual coefficients with an absolute value above the threshold were set to the median of the set of coefficients outside the artifact. This differs from typical wavelet denoising (hard, soft, or soft-like thresholding) in that it is concerned with eliminating the values above the threshold rather than below. The multilevel wavelet decomposition technique is illustrated in Fig. 6. For comparison to this process, wavelet removal was also done with the level held constant at each value from 3 through 9.

D. Quantitative Analysis of EOG Removal

Analysis of EOG Removal is a difficult process in itself. The seemingly two most obvious methods of evaluation are visual inspection and BCI decoding results. Visual inspection is effective for quick verification or with small datasets, but it is subject to human bias and error and is impractical for use on high-dimensional data. BCI decoding results are not a good criteria because the decoding algorithm could be invariant to EOG artifacts or eye movement could be biased toward a

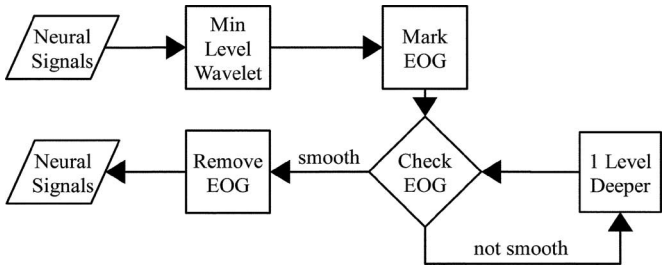

Fig. 6. Illustration of the process for determining the optimal level of wavelet decomposition. The minimum level decomposition was set at level 3. The "Check EOG" step checks the smoothness of the coefficients marked as artifactual as described in the previous paragraph.

certain class, thereby improving decoding results and giving the impression that the BCI is effective when the system is actually controlled by eye movement.

There are two main criteria that should be used to evaluate an EOG removal technique: 1) how well the artifact was removed and 2) how well the neural data were preserved. The methods used here to measure these criteria were in large part taken from previous methods given in Section II-B [10], [14], but modifications were made to improve performance and adapt to using real neural data rather than simulated. This is a key since the main difficulties in evaluating EOG removal arise with real data where the ground truth is not known.

To determine how well the neural data were preserved, a number of measures were used. For many of these measures, only those portions of the signals that were originally artifact free were used. These portions of the signal should remain the same after EOG removal. EOG artifacts were marked by low pass filtering at 10 Hz and then detecting threshold crossings. On the uncontaminated portion of the signal, correlation coefficient and Euclidean distance were used as discussed in Section II-B. The STD ratio was replaced due to a couple of pitfalls that could arise with this metric. With any average there is the potential for a result that seems good, but is actually highly skewed or multimodal. Also, use of the ratio presents the possibility that a denominator near 0 for any trial would be a large enough outlier to ruin the overall average. Instead of the STD ratio, the mean-squared difference between the STD of the original and processed signals was used. This will be referred to as the exterior STD difference.

To determine how well the artifact was removed, the main metric was the percentage of contaminated trials where an EOG artifact was still detected after the reduction process (using the filtering and thresholding method discussed in the previous paragraph). It should be noted that the absolute percentage of removed artifacts is not as important as the relative percentages between methods since the artifact detection itself is not perfect. Also, the difference between STD of the entire processed signal and that of the artifact-free portion of the original signal was calculated. This will be referred to as the total STD difference. Using the entire signal should reduce the impact of the signal's nonstationarity, and since the power of a portion of the signal can deviate to either side of the mean, taking the mean over a large number of trials should still produce a value as close to 0 as possible. Finally, the frequency correlation was examined to determine the effect of the removal process on the signal's spectrum.

IV. Results and Discussion

The datasets used here contained 306-channel MEG neural recordings, sampled at 1 kHz, of both language processes and motor functions. In the language sets, subjects are observing various words and images. Trials are 5 s long, and there are a total of 540 trials. The motor datasets contain 2.5-s trials of both overt (775 trials) and imagined (640 trials) wrist movement. All subjects had normal brain function and data collection was approved by the Institutional Review Boards of the University of Pittsburgh and Carnegie Mellon University. The different datasets were used to test EOG removal methods on data of different trial lengths and with different frequencies of each type of EOG artifact. EOG recordings were made above and lateral to the eye. It has been shown that having vertical and horizontal EOG channels produces better results than one channel [21].

Table I and Fig. 7 show the results of the quantitative performance metrics discussed in Section III-D after performing EOG removal on the aforementioned datasets. The running time of each removal process relative to the fastest method (regression) is also given. Surprisingly, regression performed well in measures of preservation of the neural data. The poor performance in removing artifacts nulls any value associated with retention of neural data, though. The removal percentage is extremely low, and the negative total STD difference indicates that not enough power was removed from the contaminated portion of the signal. These results indicate that the regression coefficients [$\boldsymbol{A}$ in (1)] are too small. Using a regression method in which the regression coefficients are calculated separately for each EOG channel might improve results, but it could not probably increase removal percentage to a satisfactory level while maintaining high preservation of neural data due to the neural contamination in EOG channels.

PCA was also inefficient in removing artifacts. This is most likely an inherent limitation of using PCA for EOG removal in that PCA was unable to fully separate the artifacts from the neural data. This is mostly due to PCA only decorrelating the data, and the requirement of spatial orthogonality of the signal components is an additional restriction that might prevent separation of artifacts from the neural components. Methods of detecting additional artifactual components or residuals distributed throughout the neural components could improve results, but such an effort would most likely not be worthwhile in light of results from other removal techniques.

ICA showed a large improvement over PCA and regression in removing artifacts. The novel distribution offset method outperformed the Hurst exponent method in identification of artifactual components. Distribution offset had a higher removal percentage, but its main advantage was that it far exceeded the Hurst exponent in preserving neural data. Since the Hurst values eliminated were associated with any noninteresting data rather than just EOG artifacts, as in [18], it is possible that the Hurst method removed additional noise, such as line noise or

TABLE I
EVALUATION OF EOG REMOVAL TECHNIQUES

METRIC	REGRESSION	PCA	ICA (DIST. OFFSET)	ICA (HURST)	WAVELET LEVEL 5	WAVELET LEVEL 4	WAVELET MULTI-LEVEL
CORRELATION COEFFICIENT (x 10^{-2})	99.0 ± 1.9	98.4 ± 2.4	96.0 ± 14	71.7 ± 35	98.3 ± 5.8	98.5 ± 5.2	98.4 ± 5.2
EUCLIDEAN DISTANCE (x 10^{-11})	2.64 ± 3.8	3.33 ± 4.3	3.51 ± 8.2	7.96 ± 11	2.37 ± 6.7	2.12 ± 6.1	2.37 ± 6.8
EXTERIOR STD DIFFERENCE (x 10^{-25})	0.25 ± 2.5	0.46 ± 4.8	20.4 ± 140	61.8 ± 190	3.02 ± 30	2.55 ± 28	2.88 ± 29
TOTAL STD DIFFERENCE (x 10^{-14})	-10.2 ± 54	-5.21 ± 53	18.1 ± 140	110 ± 220	0.67 ± 65	-2.62 ± 61	-0.53 ± 65
REMOVAL PERCENTAGE	19.9	28.7	74.3	64.7	88.5	91.2	91.3
RELATIVE COMPUTATION TIME	1.00	2.20	21.0	20.4	2.76	2.49	2.72

For the first four rows, the values are given as mean ± standard deviation.

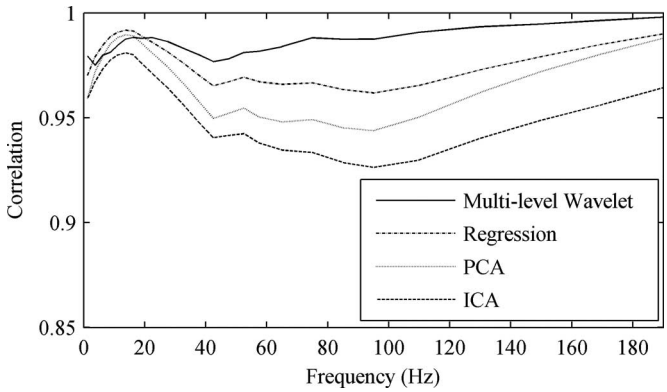

Fig. 7. Frequency correlation between original and processed signals. Here, ICA uses distribution offset for identification of artifactual components.

TABLE II
REMOVAL PERCENTAGES FOR DIFFERENT DATASETS

DATASET	REGRESSION	PCA	ICA (DIST. OFFSET)	WAVELET MULTI-LEVEL
LANGUAGE	55.51	62.03	86.08	96.42
OVERT WRIST	12.27	22.94	73.11	90.25
IMAGINED WRIST	13.49	20.91	73.12	90.37

electromyography artifacts, rather than vital neural data, but it is doubtful that the large amount of information removed could be fully accounted for by noise.

Even using distribution offset, ICA was not as effective as other methods in preserving neural data. This tradeoff was expected, and the overall results show ICA to be a much more viable option for EOG artifact removal than regression and PCA. Based on the neural preservation metrics and the positive total STD difference, ICA removes too much data, which is most likely a result of neural data not being fully separated from artifactual components. The frequency correlation graph also shows this as ICA (distribution offset method) has the smallest correlation of any removal technique.

A method that computes ICA on the full data matrix might be able to better separate the data, but on a dataset such as ours this would require concatenation of trials to obtain enough time points, which requires the assumption of spatial stationarity of the neural sources across trials. This would be a difficult assumption to make given that our trials contained different stimuli, although it should be noted that some studies have found it satisfactory to only compute the ICA unmixing matrix once with as little as 10 s of data [8]. That technique also helps alleviate ICA's large computation time.

The most effective method examined was the wavelet method. Not only did the wavelet technique produce the best results in removing EOG artifacts, but it was far superior to ICA in retaining neural data. It was also much more consistent than ICA in all measures as indicated by the STDs in Table I. Additionally, the wavelet method produced results that had the highest frequency correlation with the original signal above 20 Hz. Last, the wavelet technique has the distinct advantage of not needing the EOG reference channels, thereby decreasing experimental complexity and possible sources of error while increasing the subject's comfort.

Wavelets, along with ICA, were also more robust to the different datasets (Table II). Regression and PCA performed over 40% worse at removal in the motor datasets compared to the language set. There was no significant difference between the imagined and overt motor sets for any removal method, though, which would seem to indicate that the large drop in removal percentage from the language set was due to the change in trial length from 5 to 2.5 s.

To evaluate the effectiveness of the multilevel wavelet technique, its results were compared to the results of using wavelets with optimal constant decomposition levels, which were found to be levels 4 and 5 through the same metrics presented in Table I. Levels 4 and 5 are shown in Table I, and the multilevel method produced superior results. Although multilevel wavelets were not the best in every metric, the overall results are slightly better than any single level. As expected, the multilevel technique removed artifacts as well as level 4 decompositions as indicated by removal percentage, while still leaving behind the proper amount of power in the contaminated portion of the signal as shown by the total STD difference. The multilevel technique also saves the time of manually finding the optimal level. If the optimal level for nearly all artifacts is the same, though, then the multilevel method adds unnecessary computation time.

In visual inspection of a sample of signals, the multilevel wavelet technique again showed the best results. Fig. 8 shows typical results from multilevel wavelets in which it is clear that the noncontaminated portions of the signal were left untouched, and two types of EOG artifacts appear to have been removed while still retaining the neural data.

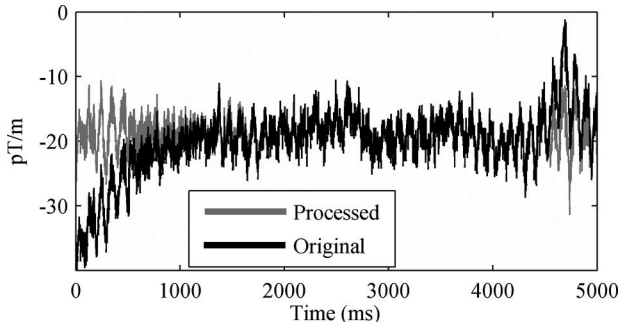

Fig. 8. EOG removal with multilevel wavelets. At the beginning of the signal, there is an eye movement artifact, and at the end of the signal an eye blink occurs. Both artifacts were removed while retaining neural data.

V. Conclusion

The main contributions of this paper are the development of a novel wavelet technique for removal of OA from neural data, a novel method for automatic identification of ocular artifact components in ICA, and a set of quantitative metrics for automatic evaluation of the effectiveness of EOG removal on real neural data. As discussed in Section IV, multilevel wavelets were most effective in terms of EOG artifact removal and preservation of neural data. This conclusion is supported by the quantitative metrics (see Table I; Fig. 7) as well as by visual inspection of a sample of signals (such as Fig. 8). This method also did not require EOG reference channels.

Although ICA encountered complications with the high-dimensional data, it has been the gold standard for EOG artifact removal in low-dimensional datasets. Here, distribution offset, the novel method that was developed for automatic artifact identification, outperformed the Hurst exponent technique in both artifact removal and preservation of neural data. Neither ICA method performed nor the wavelets, but both were far superior to regression and PCA.

Acknowledgment

The authors would like to thank G. Sudre and Dr. D. Pomerleau for collecting and providing the MEG data for this study, the Center for Advanced Brain Magnetic Source Imaging (CABMSI) at the University of Pittsburgh Medical Center for providing the scanning time for MEG data collection, and Anna Haridis at CABMSI for assistance in MEG setup and data collection. The contents of this publication do not represent the views of the Department of Veterans Affairs or the United States Government.

References

[1] T. M. Vaughan, W. J. Heetderks, L. J. Trejo, W. Z. Rymer, M. Weinrich, M. M. Moore, A. Kübler, B. H. Dobkin, N. Birbaumer, E. Donchin, E. W. Wolpaw, and J. R. Wolpaw, "Brain–computer interface technology: A review of the Second International Meeting," *IEEE Trans. Neural Syst. Rehabil. Eng.*, vol. 11, no. 2, pp. 94–109, 2003.

[2] M. Fatourechi, A. Bashashati, R. K. Ward, and G. E. Birch, "EMG and EOG artifacts in brain computer interface systems: A survey," *Clin. Neurophysiol.*, vol. 118, pp. 480–494, 2007.

[3] C. J. Ochoa and J. Polich, "P300 and blink instructions," *Clin. Neurophysiol.*, vol. 111, pp. 93–98, 2000.

[4] R. Verleger, "The instruction to refrain from blinking affects auditory P3 and N1 amplitudes," *Electroencephalogr. Clin. Neurophysiol.*, vol. 78, pp. 240–251, 1991.

[5] R. J. Croft and R. J. Barry, "Removal of ocular artifact from the EEG: A review," *Clin. Neurophysiol.*, vol. 30, pp. 5–19, 2000.

[6] B. Noureddin, P. Lawrence, and G. Birch, "Quantitative evaluation of ocular artifact removal methods based on real and estimated EOG signals," in *Proc. 30th IEEE EMBS Conf.*, 2008, pp. 5041–5044.

[7] D. J. McFarland, L. M. McCane, S. V. David, and J. R. Wolpaw, "Spatial filter selection for EEG-based communication," *Electroencephalogr. Clin. Neurophysiol.*, vol. 103, pp. 386–394, 1997.

[8] T. P. Jung, S. Makeig, C. Humphries, T. W. Lee, M. J. McKeown, V. Iragui, and T. J. Sejnowski, "Removing electroencephalographic artifacts by blind source separation," *Psychophysiology*, vol. 37, pp. 163–178, 2000.

[9] T. D. Lagerlund, F. W. Sharbrough, and N. E. Busacker, "Spatial filtering of multichannel electroencephalographic recordings through principal component analysis by singular value decomposition," *J. Clin. Neurophysiol.*, vol. 14, pp. 73–82, 1997.

[10] V. Krishnaveni, S. Jayaraman, L. Anitha, and K. Ramadoss, "Removal of ocular artifacts from EEG using adaptive thresholding of wavelet coefficients," *J. Neural Eng.*, vol. 3, pp. 338–346, 2006.

[11] T. Zikov, S. Bibian, G. A. Dumont, M. Huzmezan, and C. R. Ries, "A wavelet based de-noising technique for ocular artifact correction of the electroencephalogram," in *Proc. 2nd Joint IEEE EMBS/BMES Conf.*, 2002, vol. 1, pp. 98–105.

[12] G. Ouyang, X. Li, Y. Li, and X. P. Guan, "Application of wavelet-based similarity analysis to epileptic seizures prediction," *Comp. Biol. Med.*, vol. 37, pp. 430–437, 2007.

[13] X. Li, X. Yao, J. R. G. Jefferys, and J. Fox, "Interaction dynamics of neuronal oscillations analysed using wavelet transforms," *J. Neurosci. Methods*, vol. 160, pp. 178–185, 2007.

[14] L. Vigon, M. R. Saatchi, J. E. W. Mayhew, and R. Fernandes, "Quantitative evaluation of techniques for ocular artefact filtering of EEG waveforms," *Sci. Meas. Tech., IEE Proc.*, vol. 147, no. 5, pp. 219–228, Sep. 2000.

[15] S. Makeig *et al.* (2002–2010). "Frequently asked questions about ICA applied to EEG and MEG data," WWW Site, Swartz Center for Computational Neuroscience [Online]. Available: www.sccn.ucsd.edu/∼scott/icafaq.html

[16] A. Hyvärinen, "Fast and robust fixed-point algorithms for independent component analysis," *IEEE Trans. Neural Netw.*, vol. 10, no. 3, pp. 626–634, May 1999.

[17] T. P. Jung, S. Makeig, M. Westerfield, J. Townsend, E. Courchesne, and T. J. Sejnowski, "Removal of eye activity artifacts from visual event- related potentials in normal and clinical subjects," *Clin. Neurophysiol.*, vol. 111, no. 10, pp. 1745–1758, Oct. 2000.

[18] S. Vorobyov and A. Cichocki, "Blind noise reduction for multisensory signals using ICA and subspace filtering, with application to EEG analysis," *Biol. Cybern.*, vol. 86, pp. 293–303, 2002.

[19] N. Mammone and F. C. Morabito, "Enhanced automatic artifact detection based on independent component analysis and Renyi's entropy," *Neural Netw.*, vol. 21, pp. 1029–1040, 2008.

[20] H. Cui and G. Song, "Study of the wavelet basis selections," in *Proc. Int. Conf. Comput. Intell. Security*, Nov. 2006, vol. 2, pp. 1833–1836.

[21] T. Elbert, W. Lutzenberger, B. Rockstroh, and N. Birbaumer, "Removal of ocular artifacts from the EEG—A biophysical approach to the EOG," *Electroencephalogr. Clin. Neurophysiol.*, vol. 60, pp. 455–463, 1985.

John W. Kelly (S'04) was born in Oak Ridge, TN, in 1984. He received the B.S. degrees in both electrical and computer engineering in 2003, and the M.S. degree in electrical engineering, in 2004, both from North Carolina State University, Raleigh. He is currently working toward the Ph.D. degree in electrical and computer engineering at Carnegie Mellon University, Pittsburgh, PA.

His previous positions include multiple summer internships and a job as a Software Developer at Oak Ridge National Laboratory and a summer internship at Y-12 National Security Complex. His current research interests include neural signal processing to provide automated methods of developing and controlling brain–computer interfaces.

Mr. Kelly was the recipient of the National Defense Science and Engineering Graduate (NDSEG) Fellowship in 2008 and the NSF Graduate Research Fellowship in 2009.

Daniel P. Siewiorek (F'79) received the B.S. degree in electrical engineering from the University of Michigan, Ann Arbor, in 1968, and the M.S. and Ph.D. degrees in electrical engineering (minor in computer science) from Stanford University, Palo Alto, CA, in 1969 and 1972, respectively.

He is the Buhl University Professor of Electrical and Computer Engineering and Computer Science at Carnegie Mellon University, Pittsburgh, PA. He has designed or been involved with the design of nine multiprocessor systems and has been a key contributor to the dependability design of more than two dozen commercial computing systems. He leads an interdisciplinary team that has designed and constructed more than 20 generations of mobile computing systems. He has written nine textbooks in the areas of parallel processing, computer architecture, reliable computing, and design automation in addition to more than 475 papers. His previous positions include the Director of the Human Computer Interaction Institute, the Director of the Engineering Design Research Center, and a cofounder and the Associate Director of the Institute for Complex Engineered Systems.

Dr. Siewiorek is a Fellow of ACM and AAAS and is a member of the National Academy of Engineering. He has served as the Chairman of the IEEE Technical Committee on Fault-Tolerant Computing and as the founding Chairman of the IEEE Technical Committee on Wearable Information Systems. He is the recipient of the AAEE Frederick Emmons Terman Award, the IEEE/ACM Eckert-Mauchly Award, and the ACM SIGMOBILE Outstanding Contributions Award.

Asim Smailagic (SM'03–F'10) received the B.S. degree in electrical engineering in 1973, and the M.S. and Ph.D. degrees in computer science from the University of Sarajevo, Yugoslavia, in 1976 and 1984, respectively. He received the Postdoctoral degree in computer science from Carnegie Mellon University, Pittsburgh, PA, in 1988.

He is a Research Professor in the Institute for Complex Engineered Systems, College of Engineering, and Department of Electrical and Computer Engineering at Carnegie Mellon University (CMU). He is also the Director of the Laboratory for Interactive and Wearable Computer Systems at CMU. He has written or edited several books in the areas of mobile computing, digital system design, and VLSI systems and has given keynote lectures at over a dozen representative international conferences.

Dr. Smailagic is the Chair of the IEEE Technical Committee on Wearable Information Systems. He has been a Program Chairman or Co-Chairman of IEEE conferences more than 10 times. He has had editorship roles in the IEEE TRANSACTIONS ON MOBILE COMPUTING, PARALLEL AND DISTRIBUTED SYSTEMS, IEEE TRANSACTIONS VLSI SYSTEMS, and IEEE TRANSACTIONS COMPUTERS, and—IEEE JOURNAL ON SELECTED AREAS IN COMMUNICATIONS, *Journal on Pervasive and Mobile Computing*, etc. He received the 2000 Allen Newell Award for Research Excellence from the CMU's School of Computer Science, the 2003 Carnegie Science Center Award for Excellence in IT, and the 2003 Steve Fenves Systems Research Award from the CMU's College of Engineering. He received the Fulbright Postdoctoral Award in computer science at Carnegie Mellon University, in 1988.

Jennifer L. Collinger received the B.S. and Ph.D. degrees in bioengineering from the University of Pittsburgh, Pittsburgh, PA, in 2003 and 2009, respectively.

She is currently an Assistant Professor in the Department of Physical Medicine and Rehabilitation, University of Pittsburgh. She is also a Research Biomedical Engineer at VA Pittsburgh Healthcare System in the Department of Veterans Affairs. She is an Investigator at the Human Engineering Research Laboratories, a VA Rehabilitation Research and Development Center of Excellence for Wheelchairs and Associated Rehabilitation Engineering. Her research interests include neurorehabilitation, the study of neuroplasticity, neuroprosthetics, and brain–computer interface technology. She is interested in developing and evaluating new rehabilitation strategies or assistive technologies for individuals with motor impairments.

Dr. Collinger has been a member of the Rehabilitation Engineering Society of North America since 2003 and the Society for Neuroscience since 2008.

Douglas J. Weber (M'94) received the B.S. degree in biomedical engineering from the Milwaukee School of Engineering, Milwaukee, WI, in 1994, and the M.S. and Ph.D. degrees in Bioengineering from Arizona State University, Tempe, AZ, in 2000 and 2001, respectively.

He is currently an Assistant Professor in the Department of Physical Medicine and Rehabilitation, University of Pittsburgh, Pittsburgh, PA. He is also a Faculty Member in the Department of Bioengineering and the Center for the Neural Basis of Cognition. Previously, he was a Postdoctoral Fellow and then an Assistant Professor in the Centre for Neuroscience at the University of Alberta. His primary research area is in neural engineering, including studies of motor learning and control of walking and reaching with particular emphasis on applications to rehabilitation technologies and practice. His specific research interests include functional electrical stimulation, activity-based neuromotor rehabilitation, neural coding, and neural control of prosthetic devices. Active projects in his lab include the development of somatosensory neural interfaces (SSNI) to record from or stimulate primary afferent neurons in cats and humans, and brain machine interface studies with magnetoencephalography and electrocorticography in humans.

Dr. Weber has been a member of the IEEE Engineering in Medicine and Biology Society since 1994 and a member of the Society for Neuroscience since 1995.

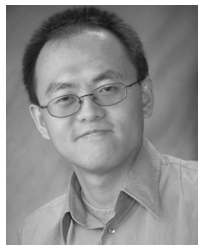

Wei Wang received the M.D. degree from Peking University Health Science Center (formerly Beijing Medical University), Beijing, China, in 1999, the M.Sc. degree in biomedical engineering from the University of Tennessee Health Science Center, Memphis, TN, in 2002, and the Ph.D. degree in biomedical engineering from Washington University, St. Louis, St. Louis, MO, in 2006.

He is currently an Assistant Professor in the Department of Physical Medicine and Rehabilitation with a secondary appointment in the Department of Bioengineering at the University of Pittsburgh, Pittsburgh, PA. Prior to joining the University of Pittsburgh, he served as a Senior Scientist at St. Jude Medical, Inc., Sylmar, CA. His research interests include neural engineering, motor neuroprosthetics, brain–computer interfaces, rehabilitation of movement disorders, and motor system neurophysiology.

Dr. Wang currently holds a multidisciplinary Clinical Research Scholar (NIH KL2) Award from the University of Pittsburgh.